

## Accepted Article

**Title:** Ultrafast light-driven substrate expulsion from the active site of a photoswitchable catalyst

**Authors:** Manuel Pescher, Luuk van Wilderen, Susanne Gruetzner, Chavdar Slavov, Josef Wachtveitl, Stefan Hecht, and Jens Breidenbeck

This manuscript has been accepted after peer review and appears as an Accepted Article online prior to editing, proofing, and formal publication of the final Version of Record (VoR). This work is currently citable by using the Digital Object Identifier (DOI) given below. The VoR will be published online in Early View as soon as possible and may be different to this Accepted Article as a result of editing. Readers should obtain the VoR from the journal website shown below when it is published to ensure accuracy of information. The authors are responsible for the content of this Accepted Article.

**To be cited as:** *Angew. Chem. Int. Ed.* 10.1002/anie.201702861  
*Angew. Chem.* 10.1002/ange.201702861

**Link to VoR:** <http://dx.doi.org/10.1002/anie.201702861>  
<http://dx.doi.org/10.1002/ange.201702861>

# Ultrafast light-driven substrate expulsion from the active site of a photoswitchable catalyst

Manuel Pescher,<sup>[+][a]</sup> Luuk van Wilderen,<sup>[+][a]</sup> Susanne Grützner,<sup>[b]</sup> Chavdar Slavov,<sup>[c]</sup> Josef Wachtveitl,<sup>[c]</sup> Stefan Hecht<sup>[b]</sup> and Jens Breckenbeck<sup>\*[a]</sup>

**Abstract:** The azobenzene-containing photoswitchable piperidine general base catalyst is a prototype structure for light control of catalysis. Its azobenzene moiety moves sterically-shielding groups to either protect or expose the active site, thereby changing the compound's basicity and hydrogen-bonding affinity. The catalyst's reversible switching dynamics is probed in the infrared spectral range by monitoring hydrogen bond (HB) formation between its active site and methanol (MeOH) as HB donor. Steady-state infrared (IR) and ultrafast IR and UV/Vis-spectroscopies are used to uncover ultrafast expulsion of MeOH from the active site within a few picoseconds. Thus, the force generated by azobenzene even in the final phase of its isomerisation is sufficient to break a strong HB within 3 ps and to shut down access to the active site.

Precise temporal and spatial control of (bio)chemical processes opens up new possibilities for applications. In recent years, a variety of molecular properties have successfully been rendered photoswitchable, for instance secondary structure formation in peptides,<sup>[1]</sup> protein function<sup>[2]</sup> or force generation in molecular motors.<sup>[3]</sup> Typically, photocontrol occurs via irreversible bond cleavage or via reversible switching.<sup>[4]</sup> The usage of light to irreversibly photodissociate and thereby activate a caged compound allows the initiation of a reaction at a defined point in time. Unfortunately the process induced by the initial cleavage cannot be reversed or shut down. This limitation is overcome by making the activation reversible and repeatable, utilizing geometric rearrangements of molecular structure. This approach has been used to photoswitch biological activity of proteins<sup>[4,5]</sup> and DNA transcription.<sup>[6]</sup> Considerable efforts are being made to reversibly photoregulate catalysis, which is perhaps the most attractive function to control from a chemist's point of view.<sup>[7]</sup> A prominent example is the previously developed azobenzene (AB) based supramolecular catalyst,<sup>[8]</sup> which brings two metal centers in proximity in the active state. Another system is a light-responsive cavitand<sup>[9]</sup> which binds and thereby activates the catalyst. Osorio-Planes et al.<sup>[10]</sup> recently reported regulation of catalytic activity via photoswitchable intramolecular HBing that inhibits the active site. Note that photoregulated

catalysis (via uncaging or photoswitching) has to be distinguished from photo-catalysis,<sup>[11]</sup> where a photoreaction is promoted by electronic excitation.

The previously developed catalyst under study (Figure 1A, blue structures),<sup>[12,13]</sup> shortly called "Azocat" (derived from AB-based catalyst), is a prototype system for conformational control of reactivity. This molecule catalyses the Henry reaction, a base-catalysed addition of nitroalkanes to aldehydes or ketones, for which reversible active-site accessibility has already been shown.<sup>[12,13]</sup> Other types of active centers can in principle be controlled in a similar fashion.

Azocat consists of four main structural moieties: the active centre, formed by a *tert*-butylpiperidine (t-BP); a linker group ( $\gamma$ -butyrolactone;  $\gamma$ -BL) providing a stiff connection between t-BP and AB due to the combination of a spiro-center and  $sp^2$ -hybridised atoms; the AB switch; and steric shields (two 2,6-dimethylbenzene groups, labeled R' in Figure 1A) blocking Azocat's active site in the closed state. Illumination with 365 nm induces *trans-cis* isomerization in the AB moiety leading to a large structural rearrangement of the system. The *cis*-form represents the open or active form of the catalyst, because the catalytic centre located at the t-BP can be accessed by reaction partners. The reverse process is triggered by wavelengths > 450 nm, bringing the shield to a proximal position and inactivating the catalyst. The back reaction occurs also thermally, but the lifetime of the open form at room temperature is several hundred hours.<sup>[13]</sup> The isomerization quantum yields of AB are about 0.4-0.5 for *cis-trans* and 0.1-0.2 for *trans-cis*.<sup>[14]</sup> In the photo-stationary state *cis/trans* and *trans/cis* ratios of 95:5 and 90:10 are achieved for Azocat.<sup>[13]</sup> Its high photostability allows for a large number of switching cycles. The t-BP moiety exhibits a nitrogen-atom with a free electron pair, making it an ideal acceptor for HBs. The formation of a strong HB to Azocat's catalytic centre explains its catalytic activity.

Here, we study the kinetics and structural changes of Azocat's switching process in absence and presence of HB-forming partners. The solvent is perchloroethylene (PCE) which is apolar and aprotic. The switching process and its interaction with a substrate (MeOH in our case, which donates a strong HB to the active site) are investigated by steady-state and time-resolved ultrafast IR and UV-Vis spectroscopies (experimental details and methods<sup>[15]</sup> in the SI) to understand the catalyst's isomerisation process followed by HB network reorganisation. The binding of MeOH to the active site can be easily followed in the IR, because the OH-stretching vibration changes upon HB formation.<sup>[16]</sup>

**Steady-State FTIR spectroscopy.** In order to understand the ultrafast structural changes of the catalyst and its environment we first discuss the steady-state FTIR spectra of Azocat, its active site mimic methylpiperidine (NMP) and of MeOH at different concentrations.

**Reversibility and isomerisation of the catalyst.** Upon illumination, Azocat isomerises reversibly, which is evident

[a] M. D. Pescher, Dr. L. J.G.W. van Wilderen, Prof. J. Breckenbeck  
Institute for Biophysics, Johann-Wolfgang-Goethe Universität  
Frankfurt am Main, Germany  
E-mail: breckenbeck@biophysik.uni-frankfurt.de

[b] S. Grützner, Prof. S. Hecht  
Department of Chemistry, Humboldt-Universität zu Berlin  
Berlin, Germany

[c] Dr. C. Slavov, Prof. J. Wachtveitl  
Institute of Physical and Theoretical Chemistry, Johann-Wolfgang-  
Goethe Universität  
Frankfurt am Main, Germany

[+] These authors contributed equally to this work.  
Supporting information for this article is given via a link at the end of  
the document.

by the symmetric FTIR difference spectra (see Figure S1). As in AB, the  $\nu\text{N}=\text{N}$  band ( $1520\text{ cm}^{-1}$ ) serves as isomerization marker, as it is only IR active in the *cis*-form due to the local point symmetry being broken upon isomerisation.

**MeOH binds to the active center in equilibrium with MeOH in solution.** MeOH can only bind to Azocat's active site in the open *cis*-state. We monitored the changes induced by HBing in the  $\nu\text{OH}$  region, as shown in the light-induced difference spectra of Azocat in Figure 1A. In absence of MeOH only  $\nu\text{CH}$  bands are visible in the region below  $3100\text{ cm}^{-1}$ . Upon addition of MeOH three bands above  $3100\text{ cm}^{-1}$  appear. The OH-band labeled with  $\xi$  is centered around  $3250\text{ cm}^{-1}$  and shows the highest induced absorption and largest fwhm (full width at half maximum).

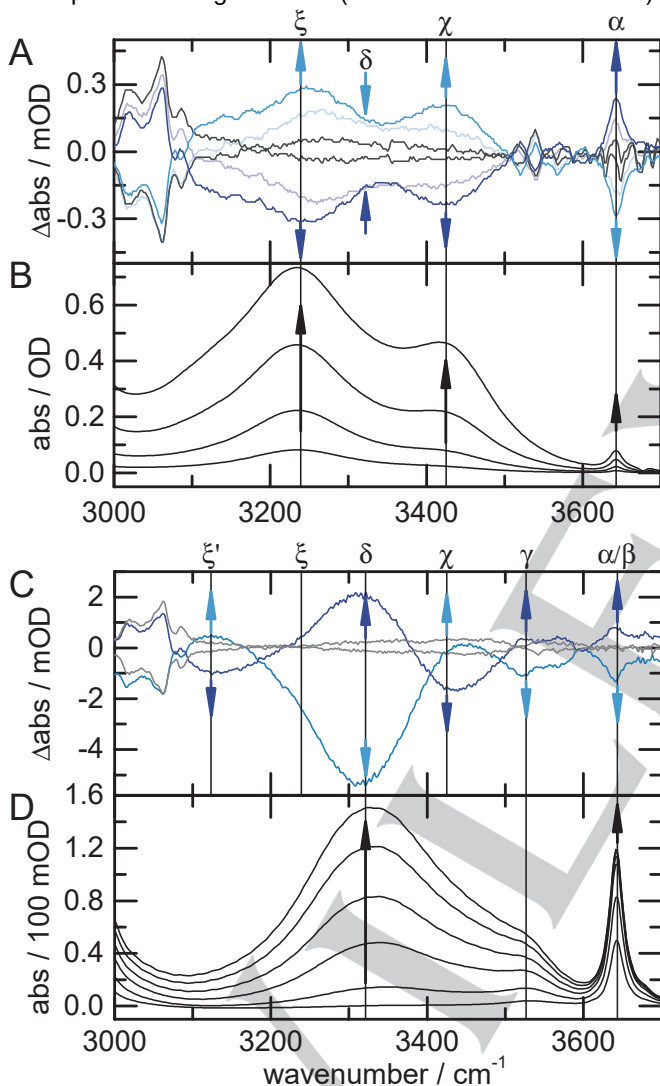
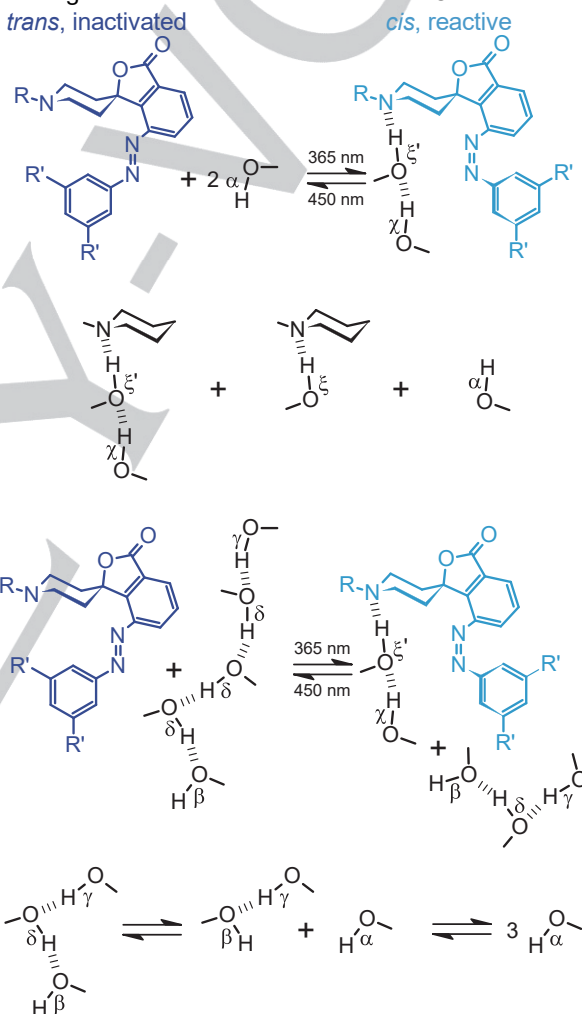


**Figure 1.** MeOH binds to the active site. Next to each FTIR spectrum, molecular structures are drawn with Greek labels corresponding to those at the vibrational bands. The arrows in all spectra denote the direction of the spectral changes due to increasing MeOH concentration. Panels A and C present the light-induced difference spectra of Azocat (with  $R = \text{tert-butyl}$  and  $R' = 2,6\text{-dimethylbenzene}$  in the structures) with low and high MeOH concentration, respectively. In the spectra after  $365\text{ nm}$  excitation (light blue) bands appearing upon formation of the reactive *cis*-form (light blue) have a positive sign. Correspondingly, in the spectra after  $450\text{ nm}$  excitation (dark blue) bands vanishing upon formation of the inactive *trans*-form (dark blue) have a negative sign. The light blue spectra have the catalytically inactive *trans*-form subtracted, the dark blue that of the reactive *cis*-form. Panels B and D show the absorption spectra of increasing MeOH concentration in the presence and absence of NMP, respectively. Concentrations: A) Azocat ( $2\text{ mM}$ ) is switched in the absence (gray) and presence of MeOH ( $49\text{ mM}$ ; light blue, and  $166\text{ mM}$ ; blue). B) MeOH is added stepwise to NMP ( $1\text{ M}$ ) in PCE, mimicking the occupation of Azocat's active site. MeOH concentrations are:  $33\text{ mM}$ ,  $98\text{ mM}$ ,  $228\text{ mM}$ ,  $420\text{ mM}$  C) A higher MeOH concentration ( $685\text{ mM}$ ) in presence of Azocat ( $69\text{ mM}$ ) provides a pool of MeOH clusters that can supply MeOH to form an HB to Azocat. D) MeOH is added to pure PCE. MeOH concentrations are:  $66\text{ mM}$ ,  $131\text{ mM}$ ,  $163\text{ mM}$ ,  $196\text{ mM}$ ,  $228\text{ mM}$ ,  $260\text{ mM}$ .

The band labeled  $\chi$  at about  $3425\text{ cm}^{-1}$  is less intense and has a reduced fwhm. The highest-wavenumber absorption band ( $\alpha/\beta$ ) at  $3643\text{ cm}^{-1}$  is the narrowest and smallest. Bands  $\xi$  and  $\chi$  appear upon UV-irradiation while the  $\alpha/\beta$ -band concomitantly disappears. Therefore, the  $\xi/\chi$  and  $\alpha/\beta$  bands are interpreted as interconverting OH-species. The difference between the integral over the  $\alpha/\beta$  band and that of the  $\xi/\chi$  bands is attributed to a significant increase of the transition dipole moment upon HB formation.

To check if the observed spectral changes originate from MeOH binding to the active site, MeOH was titrated to the active-site mimic NMP in PCE (Figure 1B). NMP itself does not absorb in the  $\nu\text{OH}$  spectral region, so any observed changes are due to the added MeOH. The absorption *trans*, inactivated



spectra show the same three spectral features as those observed in Azocat in presence of MeOH. The titration shows that the  $\xi$ -band at  $3250\text{ cm}^{-1}$  grows in first, after which a band at  $3425\text{ cm}^{-1}$  appears (the  $\chi$ -band) with higher MeOH concentrations. In addition, a narrow band (the  $\alpha/\beta$ -band) at  $3643\text{ cm}^{-1}$  increases. In agreement with the interpretation in Glew and Rath's work<sup>[17]</sup> we assign the  $\alpha/\beta$ -band to free MeOH molecules. The  $\alpha$ -band represents the monomeric MeOH, while the  $\beta$ -band is due to the OH serving as a HB acceptor. Due to the small spectral separation the two bands cannot be distinguished here. The  $\xi$ -band that is formed first represents N-bound MeOH molecules. When a second MeOH binds to the N-bound  $\xi$ -MeOH, the  $\nu\text{OH}$  of the second MeOH results in the  $\chi$  band (Figure 1B, right panel).<sup>[17,18]</sup> Furthermore, a shoulder  $\xi'$  appears on the red side of the  $\xi$  band, due to former  $\xi$  species now being HB donor as well as acceptor.

The difference spectra of Azocat (see Figure 1A) basically exhibit the same features as MeOH binding to NMP, which we therefore interpret as MeOH binding to the active site (evident by the disappearance of free MeOH and by the appearance of bound MeOH showing  $\xi$ ,  $\xi'$  and  $\chi$  bands). The large redshift of the OH-stretching wavenumber of about  $400\text{ cm}^{-1}$  between free MeOH ( $\alpha$  band) and MeOH bound to the N-atom of the piperidine moiety ( $\xi$  band) corresponds to the formation of a strong HB (binding enthalpy of about 20-25 kJ/mol), both in Azocat as well as in the active site mimic NMP.<sup>[19]</sup>

**At higher MeOH concentration MeOH clusters are formed.** When switching at higher concentrations of MeOH (Figure 1C), clusters or chains of MeOH molecules are the predominant species. To compare the spectral signatures of these species to the difference signals caused by switching of Azocat, the spectra of a titration of pure MeOH to PCE are shown in Figure 1D. In agreement with previous studies<sup>[17,18]</sup> the  $\delta$ -band at  $3333\text{ cm}^{-1}$  is assigned to HB chain formation of MeOH molecules, where MeOH accepts as well as donates HB's. MeOH chains truncate at the  $\beta$  and  $\gamma$ -groups (see right panel in Figure 1D for schematic molecular configurations). The  $\gamma$ -band appears at  $3527\text{ cm}^{-1}$ , while the  $\beta$ -band overlaps with the  $\alpha$ -band of the MeOH monomers at  $3643\text{ cm}^{-1}$ . Due to HBs at the chain's end being weaker, formation of rings and long chains is preferred.<sup>[17]</sup> Upon *trans-cis* isomerization (i.e. activation, see Figure 1C), MeOH is recruited from these different species. Concomitant with the disappearance of the  $\alpha/\beta$ -band at  $3643\text{ cm}^{-1}$ , a big negative signal is observed for the  $\delta$ -band at  $3333\text{ cm}^{-1}$  (see also Fig. 1A, where at 166 mM MeOH the onset of the negative  $\delta$ -band can be seen), in addition to a smaller negative signal of the  $\gamma$ -band at  $3527\text{ cm}^{-1}$ . This  $\gamma$  band is not observed upon switching at lower MeOH concentrations (Figure 1A). The negative bands are partially compensated by the  $\chi$  and  $\xi$ -bands that are formed due to HBing of MeOH to the active site of Azocat. Note that the absorption cross-section for MeOH in clusters is larger than that for MeOH involved in N-coordination (compare Figures 1B and 1D): 33 mM of MeOH with an excess of NMP results in 0.08 mOD at the  $\xi$ -band (Figure 1B), while adding the same to a solution containing already a large amount of MeOH leads to an increase of 0.38 of the  $\delta$ -band (Figure 1D, change from 196 mM

to 228 mM). The difference signal of Azocat at high MeOH concentrations is thus attributed to a superposition of the  $\alpha/\beta$ ,  $\gamma$ ,  $\delta$ ,  $\chi$  and  $\xi$ -bands. The MeOH molecules that bind to Azocat's active site therefore originate from the different MeOH cluster species as well as from monomers and dimers. Upon switching from *cis* to *trans*, these species are repopulated by MeOH expelled from the active site.

In summary, at low MeOH concentrations MeOH targeting the active site is mainly recruited from MeOH monomers. At higher concentrations the Azocat-bound MeOH molecules are also recruited from the MeOH clusters. Inactivation of the catalyst due to *cis-trans* isomerization reverses the process, and all binding-site bound MeOHs detach.

**Ultrafast spectroscopy.** In order to investigate the expulsion process of molecules that are bound to the catalyst's active site in real time we performed ultrafast laser experiments.

**Isomerization of the catalyst.** The isomerization reaction of Azocat can be followed by tracking the  $\nu\text{N}=\text{N}$  vibration (Figure S2).<sup>[20]</sup> We observe the disappearance of the  $\nu\text{N}=\text{N}$  band (bright green trace in Figure S3) within the laser pulse, indicating immediate isomerization of the AB moiety. The ultrafast dynamics were also probed by UV-Vis spectroscopy (see Figure S4 and Figure S5). The UV-Vis difference spectra essentially show the same dynamics of Azocat without MeOH and with an excess of MeOH. This indicates that MeOH is not modulating the isomerization process.

**MeOH expulsion.** Figure 2 shows time-resolved IR spectra of the  $\nu\text{OH}$  region of a solution of Azocat and MeOH in PCE. Upon *cis-trans* isomerization of the Azocat, a positive signal appears at the  $\alpha/\beta$  monomer band, concomitant with negative signals in the range of HBed MeOH. At 2 ps a negative signal appears at the  $\xi$  species (the black spectrum), reporting the expulsion of MeOH from the active site. Like in the FTIR spectra of Figure 1A and C, three main bands ( $\alpha/\beta$ ,  $\delta$  and  $\xi$ ) are observed in Figure 2. The  $\chi$ -band is probably covered by the broad  $3200\text{ cm}^{-1}$ - $3500\text{ cm}^{-1}$  feature, belonging to the  $\delta$ -species. The  $\delta$ -band, representing MeOH clusters, has the opposite sign with respect to the FTIR results (Figure 1C). This is due to the heating induced by the pump pulse, which breaks up MeOH clusters after the heat has been dissipated from Azocat into the solution. In the steady-state switching experiments the  $\delta$ -band is positive because the signal is dominated by MeOH molecules that are released from the active site and join the MeOH clusters. The observed signal size is in line with an estimated<sup>[21]</sup> temperature rise of a few tenths of K (see SI). To further investigate the dynamics we carried out the experiment for different MeOH concentrations and plotted the integral of the free OH band for each concentration (Figure 3A). The MeOH monomer band appears instantaneously (within the pulse duration, see Figure 3B, blue curve) for all MeOH concentrations investigated. Without MeOH the integral remains essentially zero, thereby providing an internal validation for the used integration method. With MeOH a plateau appears after 3 ps that lasts up to 100 ps, with only a slight decrease after 10 ps. This slight decay may be due to the integral borders not matching the  $\alpha/\beta$  band perfectly. In order to avoid overestimation of the integral the borders were set conservatively. The integrals'

plateau height depends on the concentration of Azocat and MeOH. It approximately doubles in size upon doubling the MeOH concentration (going from 0.04 OD·cm<sup>-1</sup> at 4 ps for 41 mM MeOH to 0.08 OD·cm<sup>-1</sup> at 82 mM MeOH), while keeping the Azocat concentration at 35 mM. Further increasing the MeOH concentration to 120 mM has no effect on the plateau's height. While the uncertainty in the amplitude precludes a detailed quantitative analysis, this implies that saturation is reached in the range of about 120 mM. Therefore, no further MeOH molecules can bind to the active site in the catalyst's *cis*-configuration and get expelled upon isomerisation to the *trans*-form. This hypothesis is confirmed by the fact that an increase of the Azocat concentration from 35 mM to 54 mM with co-increasing the MeOH concentration to 200 mM leads to considerable increase of the signal again. As now more Azocat molecules are available that can form HBs to MeOH molecules in the *cis*- conformation, more MeOH is expelled from the binding site upon switching. A contribution to the free MeOH signal could arise from MeOH clusters in the vicinity of Azocat, which are dissociated by Azocat's motion. However, a simple molecular volume estimate for 54 mM Azocat (diameter about 1.2 nm) suggests only about 0.06 MeOH molecules being in the vicinity of one Azocat molecule (in addition to the one MeOH bound to the active site), even at 200 mM MeOH. The probability of a MeOH cluster being near Azocat is thus small. We conclude that destruction of clusters by the motion of Azocat does not play a role.

On longer time scales (between 100 ps and 3 ns) the integral of the  $\alpha/\beta$ -band stays constant for MeOH concentrations up to 82 mM (with the Azocat concentration remaining constant at 35 mM). However, higher MeOH concentrations of 120 mM and 200 mM lead to a continuous growth of the integral from 100 ps onwards. The higher the MeOH concentration, the higher is the increase of the integral at later time points. As shown in Figure 1D, this is the concentration range where the concentration of MeOH clusters ( $\delta$  band) starts to rise.

Control experiments using the alcohol 2,2,2-trifluoroethanol (TFE) instead of MeOH show very similar kinetics and concentration dependences (Figure S8), showing that Azocat is able to break the HB of an even stronger HBing partner (the

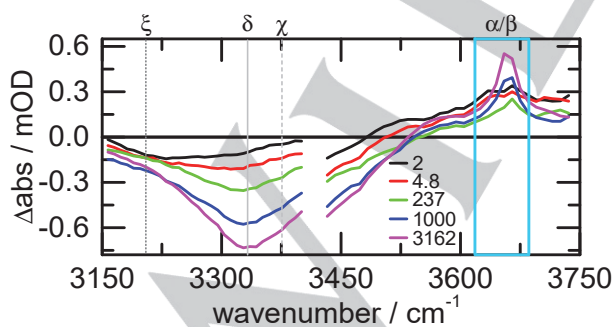


**Figure 2.** Selection of ultrafast pump-probe difference spectra upon *cis-trans* switching in the vOH region of a mixture of 200 mM MeOH and 54 mM Azocat. The small difference in signal size in the two separately measured spectral windows is caused by different spatial overlap. The delay times are given in ps. The integral of the  $\alpha/\beta$  band (light blue box) is shown in Figure 3A. The time courses at 3205 cm<sup>-1</sup> (dotted) and 3376 cm<sup>-1</sup> (dashed) are shown in Figure 3B. The grey line at 3333 cm<sup>-1</sup> depicts the position of the cluster species  $\delta$ .

redshift of the OH-stretching vibration upon HBing is 500 cm<sup>-1</sup> as compared to 400 cm<sup>-1</sup> in MeOH). The most significant difference is that the signal rise after 100 ps already sets in at lower concentrations for TFE than for MeOH, consistent with the fact that TFE starts to form clusters at lower concentrations than MeOH. The time traces of the bands  $\xi$  and  $\chi/\delta$ , which represent HBed MeOH molecules (see Figure 3B) show dynamics that nicely fit to that of the  $\alpha/\beta$  band of free MeOH. The  $\xi$ -trace, which is due to MeOH at the active site, depletes already during the IRF and then stays constant. The  $\chi/\delta$ -trace, (mainly representing MeOH clusters, in addition to contributions of N-bound MeOH) also shows a similar fast decrease, but it exhibits another strong decrease after 100 ps. This kinetics occurs in parallel with the slow appearance of additional free MeOH, confirming that it originates from the clusters. QM/MM studies of AB in the condensed phase have revealed that the initial sub-picosecond *cis-trans* isomerisation event involving the central CN=NC moiety is only weakly affected by the solvent,<sup>[22]</sup> while the subsequent orientational relaxation of the rings and the approach to the *trans*-minimum are considerably slowed down by the solvent with respect to the gas phase. In Azocat, the steric shields, which have to be moved by the AB moiety, are expected to decelerate the process further. Our experiment reveals that the switching process nevertheless rapidly creates sufficient strain to break the strong HB between the alcohol and the piperidine base and to push MeOH and TFE from the binding site within the first 3 ps as reported by the fast rise of the  $\alpha/\beta$  band and the depletion of  $\xi$  and  $\chi$  (Figure 3). At higher alcohol concentrations, where the alcohol starts to form aggregates, an additional slower (> 100 ps) generation of free alcohol can be

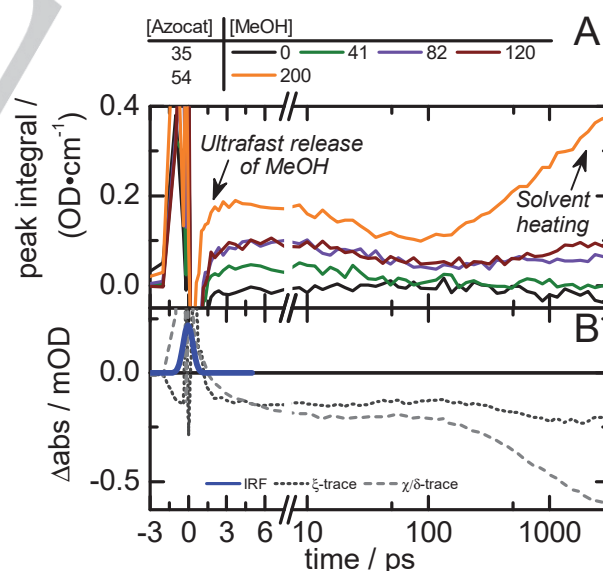


**Figure 3.** Band integral of the  $\alpha/\beta$  MeOH monomer band (panel A) as a function of time after switching Azocat to the *cis* state (closed). The experiment is carried out in the absence and presence of different concentrations of MeOH in PCE. The  $\alpha/\beta$  band appears during the pump pulse. Panel B shows the time traces of the highlighted  $\xi$  and  $\chi$  wavenumbers in Figure 2 (as dotted and dashed lines, respectively), although the latter reflects both  $\chi/\delta$  species. In blue, the IRF of the laser experiment is shown. The time scale is linear up to 7.5 ps, and logarithmic thereafter.

observed that we attribute to release of alcohol from the aggregates due to the temperature increase of the sample upon VIS excitation, shifting the equilibrium from aggregates to free alcohol. This is supported by the depletion of the  $\delta$  band at later times and the synchronous increase of the  $\alpha/\beta$  band. A similar time scale for the rise of temperature and homogeneous distribution of heat in a solution heated via laser excitation of a dye has been previously reported.<sup>[23]</sup> It is noted that only OH stretch vibrations contribute to this wavenumber range, i.e. signals of potential slow conformational equilibration dynamics of other structural moieties can be excluded, as they would appear in the transient for 0 mM MeOH in Figure 3A.

Using ultrafast and steady-state IR spectroscopy we have characterised the photoswitching and substrate binding behavior of Azocat. The ultrafast switching process makes the photoswitchable base an interesting tool for the study of chemical reactions which are difficult to time control otherwise. The binding of MeOH (via an HB) to its active site is used as a probe of Azocat's active site accessibility and thus its availability for catalysis. FTIR difference spectroscopy shows the release of MeOH upon Azocat isomerisation. In time-resolved IR measurements we observe an ultrafast release of active site-bound MeOH molecules. This shows that the force generated by the azobenzene is sufficient to break a strong HB within 3 ps, even during the final structural rearrangements of the isomerisation when the azobenzene geometry approaches the *trans* minimum of the energy surface and shuts down access to the binding site. These findings on the dynamics will aid and inspire the design of future ultrafast photoswitchable systems for applications in catalysis, mechanochemistry, and pharmacology.

## Acknowledgements

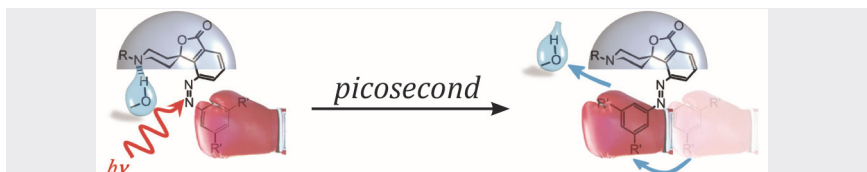
We thank Ernst Winter and Viktor Schäfer for technical support. The German Research Foundation (DFG, Grant WA 1850/4-2 and SPP 1179) is gratefully acknowledged.

**Keywords:** azobenzene • IR spectroscopy • hydrogen bonds • isomerization • femtosecond spectroscopy

- [1] a) J. Bredenbeck, J. Helbing, J. R. Kumita, G. A. Woolley, P. Hamm, *Proc. Natl. Acad. Sci. U.S.A.* **2005**, *102*, 2379; b) A. A. Deeg, M. S. Rampp, A. Popp, B. M. Pilles, T. E. Schrader, L. Moroder, K. Hauser, W. Zinth, *Chem. Eur. J.* **2014**, *20*, 694.
- [2] a) A. A. Beharry, G. A. Woolley, *Chem. Soc. Rev.* **2011**, *40*, 4422; b) A. Rullo, A. Reiner, A. Reiter, D. Trauner, E. Y. Isacoff, G. A. Woolley, *Chem. Comm.* **2014**, *50*, 14613.
- [3] a) B. L. Feringa, N. Koumura, R. A. van Delden, M. K. J. ter Wiel, *Appl. Phys. A* **2002**, *75*, 301; b) E. R. Kay, D. A. Leigh, F. Zerbetto, *Angew. Chem. Int. Ed.* **2007**, *46*, 72; c) A. Khan, C. Kaiser, S. Hecht, *Angew. Chem. Int. Ed.* **2006**, *45*, 1878; d) M. R. Panman, P. Bodis, D. J. Shaw, B. H. Bakker, A. C. Newton, E. R. Kay, A. M. Brouwer, W. J. Buma, D. A. Leigh, S. Woutersen, *Science* **2010**, *328*, 1255.
- [4] G. Mayer, A. Heckel, *Angew. Chem. Int. Ed.* **2006**, *118*, 5020.
- [5] S. Samanta, G. A. Woolley, *ChemBiochem.* **2011**, *12*, 1712.
- [6] S. Shimizu-Sato, E. Huq, J. M. Tepperman, P. H. Quail, *Nature biotechnology* **2002**, *20*, 1041.
- [7] a) V. Blanco, D. A. Leigh, V. Marcos, *Chem. Soc. Rev.* **2015**, *44*, 5341; b) R. Gostl, A. Senf, S. Hecht, *Chem. Soc. Rev.* **2014**, *43*, 1982; c) R. S. Stoll, S. Hecht, *Angew. Chem. Int. Ed.* **2010**, *49*, 5054; d) E. Léonard, F. Mangin, C. Vilette, M. Billamboz, C. Len, *Catal. Sci. Technol.* **2016**, *6*, 379; e) M. Vlatkovic, B. S. L. Collins, B. L. Feringa, *Chem. Eur. J.* **2016**, *22*, 17080.
- [8] R. Cacciapaglia, S. Di Stefano, L. Mandolini, *J. Am. Chem. Soc.* **2003**, *125*, 2224.
- [9] O. B. Berryman, A. C. Sather, A. Lledó, J. Rebek, *Angew. Chem. Int. Ed.* **2011**, *50*, 9400.
- [10] L. Osorio-Planes, C. Rodriguez-Esrich, M. A. Pericas, *Org. Lett.* **2014**, *16*, 1704.
- [11] a) A. J. Esswein, D. G. Nocera, *Chem. Rev.* **2007**, *107*, 4022; b) G. Palmisano, V. Augugliaro, M. Pagliaro, L. Palmisano, *Chem. Comm.* **2007**, 3425.
- [12] M. V. Peters, R. S. Stoll, A. Kühn, S. Hecht, *Angew. Chem. Int. Ed.* **2008**, *47*, 5968.
- [13] R. S. Stoll, M. V. Peters, A. Kuhn, S. Heiles, R. Goddard, M. Bühl, C. M. Thiele, S. Hecht, *J. Am. Chem. Soc.* **2009**, *131*, 357.
- [14] G. Zimmerman, U.-j. Paik, L.-Y. Chow, *J. Am. Chem. Soc.* **1958**, *80*, 3528.
- [15] a) J. Bredenbeck, P. Hamm, *Rev. Sci. Instrum.* **2003**, *74*, 3188; b) P. Hamm, R. A. Kaindl, J. Stenger, *Opt. Lett.* **2000**, *25*, 1798; c) C. Slavov, H. Hartmann, J. Wachtveitl, *Anal. Chem.* **2015**, *87*, 2328.
- [16] a) J. B. Asbury, T. Steinel, C. Stromberg, K. J. Gaffney, I. R. Piletic, M. D. Fayer, *J. Chem. Phys.* **2003**, *119*, 12981; b) J. B. Asbury, T. Steinel, M. D. Fayer, *J. Lumin.* **2004**, *107*, 271.
- [17] D. N. Glew, N. S. Rath, *Can. J. Chem.* **1971**, *49*, 837.
- [18] K. J. Gaffney, P. H. Davis, I. R. Piletic, N. E. Levinger, M. D. Fayer, *J. Phys. Chem. A* **2002**, *106*, 12012.
- [19] a) R. S. Bhatta, P. P. Iyer, A. Dhinojwala, M. Tsige, *Mod. Phys. Lett. B* **2014**, *28*, 1430014; b) G. C. Pimentel, A. L. McClellan, *Annu. Rev. Phys. Chem.* **1971**, *22*, 347; c) A. A. Stolov, M. D. Borisover, B. N. Solomonov, *J. Phys. Org. Chem.* **1996**, *9*, 241.
- [20] P. Hamm, S. M. Ohline, W. Zinth, *J. Chem. Phys.* **1997**, *106*, 519.
- [21] S. Chen, I. Y. S. Lee, W. A. Tolbert, X. Wen, D. D. Dlott, *J. Phys. Chem.* **1992**, *96*, 7178.
- [22] a) M. Böckmann, N. L. Doltsinis, D. Marx, *Phys. Rev. E* **2008**, *78*, 36101; b) M. Böckmann, N. L. Doltsinis, D. Marx, *J. Phys. Chem. A* **2010**, *114*, 745.
- [23] C. M. Phillips, Y. Mizutani, R. M. Hochstrasser, *Proc. Natl. Acad. Sci. U.S.A.* **1995**, *92*, 7292.

## Entry for the Table of Contents

## COMMUNICATION



Manuel Pescher, Luuk van Wilderen,  
Susanne Gruetzner, Chavdar Slavov,  
Josef Wachtveitl, Stefan Hecht and Jens  
Bredenbeck\*

Page No. – Page No.

**Ultrafast light-driven substrate expulsion from the active site of a photoswitchable catalyst**

Switching of the azobenzene moiety moves the steric shielding groups on an ultrafast time scale, expelling a strongly hydrogen bonded binding partner from the active site. The catalyst is deactivated by blocking access to the binding site.